NANO LETTERS

Letter

pubs.acs.org/NanoLett

Sodium Ion Insertion in Hollow Carbon Nanowires for Battery Applications

Yuliang Cao,*[,†,‡] Lifen Xiao,[†,§] Maria L. Sushko,[†] Wei Wang,[†] Birgit Schwenzer,[†] Jie Xiao,[†] Zimin Nie,[†] Laxmikant V. Saraf,[†] Zhengguo Yang,[†] and Jun Liu*[,†]

[†]Pacific Northwest National Laboratory, 902 Battelle Boulevard P.O. Box 999, Richland, Washington 99352, United States

[‡]Hubei Key Laboratory of Electrochemical Power Sources, College of Chemistry and Molecular Science, Wuhan University, Wuhan, 430072, P. R. China

[§]College of Chemistry, Central China Normal University, Wuhan 430079, P. R. China

Supporting Information

ABSTRACT: Hollow carbon nanowires (HCNWs) were prepared through pyrolyzation of a hollow polyaniline nanowire precursor. The HCNWs used as anode material for Na-ion batteries deliver a high reversible capacity of 251 mAh g^{-1} and 82.2% capacity retention over 400 charge−discharge cycles between 1.2 and 0.01 V (vs Na^+/Na) at a constant current of 50 mA g^{-1} (0.2 C). Excellent cycling stability is also observed at an even higher charge−discharge rate. A high reversible capacity of 149 mAh g^{-1} also can be obtained at a current rate of 500 mA g^{-1} (2C). The good Na-ion insertion property is attributed to the short diffusion distance in the HCNWs and the large interlayer distance (0.37 nm) between the graphitic sheets, which agrees with the interlayered distance predicted by theoretical calculations to enable Na-ion insertion in carbon materials.

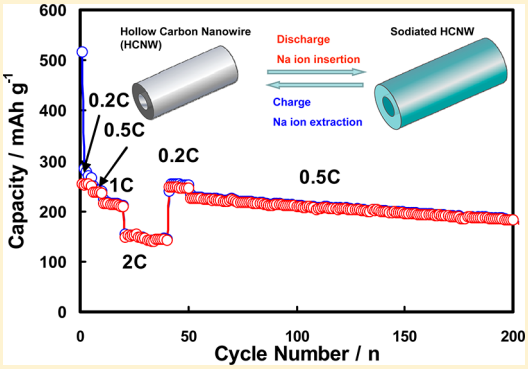

KEYWORDS: *Hollow carbon nanowires, polyaniline nanowires, anode, sodium ion battery*

Electrical energy storage has attracted wide attention for the electrification of transportation and renewable energy integration. Currently lithium ion batteries are considered one of the most promising technologies due to their long lifetime and high energy density.[1,2] However, for large-scale applications, there is increasing concern about the cost and the limitation of lithium terrestrial reserves.[3,4] As a result, great efforts have been made to explore new low-cost and reliable electrochemical energy storage technologies.

Because of the abundant supply and widespread terrestrial reserves of Na mineral salts, Na-ion batteries have attracted increasing attention as a low-cost alternative to Li-ion batteries. However, the progress of Na-ion batteries has been slow because of the lack of appropriate active materials for both cathodes and anodes. Since the Na ion is about 55% larger than the Li ion, most materials do not have sufficiently big interstitial space within their crystallographic structure to host Na ions. This greatly limits the range of potential candidate materials. There are a few materials such as manganese oxides that have large open tunnels to accommodate Na ions for cathode material, but they exhibit poor stability and reversibility for the Na insertion−extraction reaction.[5,6] Recently, several groups have made good progress on cathode material development.[7−15] Johnson et al. reported a Na layered transition metal oxide that can deliver a stable capacity of ∼95 mAh g^{-1} after 50 cycles owing to the stabilizing effect of Li doping in the layered structure.[7] Our group reported that single crystalline $Na_4Mn_9O_{18}$ nanowires offered a high reversible capacity of 128 mAh g^{-1} at first cycle (at 0.1 C) and exhibited unprecedented cyclability (77% capacity retention for 1000 cycles at 0.5 C).[8] Komaba et al. recently reported that P2−$Na_{2/3}[Fe_{1/2}Mn_{1/2}]O_2$ can deliver a higher reversible capacity of 190 mAh g^{-1} at a rate of 12 mA g^{-1} in the voltage range of 1.5−4.3 V.[14] These advances have demonstrated the feasibility of the Na-ion battery technology.

On the anode side, most studies focused on hard carbon materials due to their large interlayer distance and disordered structure, which facilitates Na-ion insertion−extraction.[16−20] Dahn and Stevens found that hard carbon from pyrolyzed glucose had an initial reversible capacity as high as 300 mAh g^{-1}, but they also pointed out that a large portion of the capacity came from the stripping of the Na metal plated onto the nanopores during discharge since the discharge cutoff voltage is set below 0 V.[16] Tirado's group reported that carbon black had a reversible capacity close to 200 mAh g^{-1}. However, the large irreversible capacity (∼70%) is still a problem.[17] Later, the same group used carbon microspheres prepared from resorcinol-formaldehyde and obtained an initial reversible

Received: May 5, 2012
Revised: May 29, 2012
Published: June 11, 2012

capacity of 285 mAh g^{-1}, but they only reported the results of limited charge–discharge cycles.[18] Recently, Komaba et al. reported another hard carbon material that could deliver a reversible capacity of about 240 mAh g^{-1} between 0 and 2 V at a current rate of 25 mA g^{-1} and maintain more than 200 mAh g^{-1} over 100 cycles.[21] Overall, these hard carbon materials have displayed capacities of 200–300 mAh g^{-1}, but there have been few reports of good cycling stability during extended operation, in particular at high charge–discharge rates.

Nanostructured materials such as nanowires/nanotubes have provided new opportunities to improve the properties of energy storage materials for various batteries because of their structural stability and good conducting connectivity.[22−25] Herein, we report hollow carbon nanowires (HCNWs) by direct pyrolyzation of a hollow polyaniline nanowire precursor. This novel carbon nanostructure displayed a high reversible capacity (251 mAh g^{-1} at 50 mA g^{-1}) and good excellent cycling stability over 400 cycles. A reversible capacity of over 200 mAh g^{-1} and more than 90% capacity retention was obtained at 125 mA g^{-1} after 200 cycles. Even at 500 mA g^{-1} (2 C) a high reversible capacity of 149 mAh g^{-1} also can be observed. From theoretical calculations, we showed that a critical minimum spacing of 0.37 nm between the graphitic layers is required to enable good Na-ion insertion properties, which agrees well with experimental observations.

The hollow polyaniline nanowires (PANI-HNWs) were prepared through self-assembly.[26−28] The amphipathic D,L-tartaric acid molecules first self-assembled to form wire-like micelles to act as a template. Then the aniline molecules underwent orientational polymerization and growth on the surface of the micelles. After the amphipathic templating molecules were washed off, polyaniline with a hollow nanowire structure was obtained. The as-prepared precursor exhibits a uniform tube-like structure with about 150 nm in diameter, about several micrometers in length (Figure 1a,b) and a 20 nm inside diameter. Higher magnification shows that the surface of the nanowires is very rough, with many nanohemispheres protruding from the surface (Figure 1b), which increases the specific surface area and the contact area with electrolyte. Scanning electron microscopy (SEM) images of the nanowire edges reveals that these nanowires have a hollow structure (inset in Figure 1a), which is also confirmed by the high-resolution transmission electron microscopy (HRTEM) characterization (Figure 1e). The diameter of the internal hollow tube is about 30 nm. In addition, the HRTEM image shows that the walls of the nanowires are filled with nanoparticles and the protrusions on the surface are embedded in the walls (Figure 1e).

After being carbonized at 1150 °C for 6 h, the material still maintains a hollow nanowire structure; however, the surface becomes smoother, and the diameter decreases slightly (Figure 1d). The TEM image in Figure 1f shows that the internal hollow tubes have a diameter of 20–40 nm. To avoid confusion with traditional carbon nanotubes, the new materials are called hollow carbon nanowires (HCNWs) in this paper. The HRTEM image in Figure 1g shows that the product consists of graphite microcrystallites, which assemble to form many disordered microvoids. The graphite microcrystallites are formed by 3–4 layer-stacked-graphene sheets. The average spacing between the graphene layers is about 0.37 nm (Figure 1g). The X-ray diffraction (XRD) patterns for the samples before and after carbonization are shown in Figure 2a. The hollow polyaniline nanowire precursor shows two broad peaks

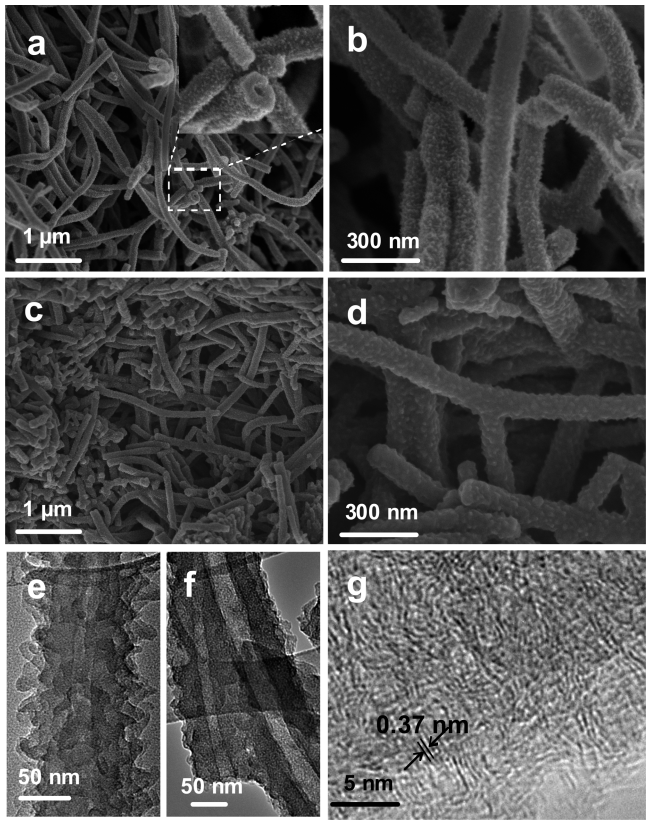

Figure 1. SEM images of the PANI-HNWs (a, b) and HCNWs (c, d). TEM images of the PANI-HNWs (e) and HCNWs (f). (g) High-resolution TEM images of the HCNWs.

centered at 2θ = 20.2° and 25.5°, which are attributed to the periodicity parallel and perpendicular to the polyaniline chains, indicating an amorphous phase.[21,26,29] After heat treatment, the XRD pattern of the HCNWs shows two broad peaks around 2θ = 24.3° and 44.4°, corresponding to the (002) diffraction of the graphitic layer-by-layer structure and the (101) diffraction for graphite, respectively. From the 2θ degree of the (002) peak, the interlayer distance ($d_{(002)}$) of graphitic layers is calculated to be 0.37 nm, which is in good agreement with the HRTEM observation in Figure 1g. Based on the full width at half-maximum (fwhm) of the (002) and (101) diffraction peaks, the *c*-axis length (L_c) and *a*-axis length (L_a) in the graphite lattice can be estimated to be 1.27 nm and 2.12 nm, respectively. Thus, the XRD results suggest that the carbonized product is composed of disordered graphite nanocrystallites with 3–4 (1.27/0.37 = 3.4) layer-stacked-graphene sheets, in agreement with the HRTEM observation in Figure 1g. The microstructure of HCNWs is illustrated in Figure 2b.[30]

Na-ion insertion–extraction behavior in HCNWs was investigated by cyclic voltammetry (CV) and galvanostatic charge–discharge cycling. To better understand the Na-ion insertion mechanism in HCNWs, the Li-ion insertion behavior in HCNWs was also conducted for comparison. The CV curves of the HCNWs electrode in the Li-ion electrolyte (Figure S1, Supporting Information (SI)) are similar to other hard carbon electrodes.[31] In the first negative scan, two irreversible reductive peaks occur at higher potentials (~1.0 and 0.7 V), which are known to reflect the decomposition of the electrolyte and the formation of solid electrolyte interphase (SEI) on the surface of carbon grains.[18,32] Figure 3a shows the CV curves of the

dx.doi.org/10.1021/nl3016957 | *Nano Lett.* 2012, 12, 3783–3787

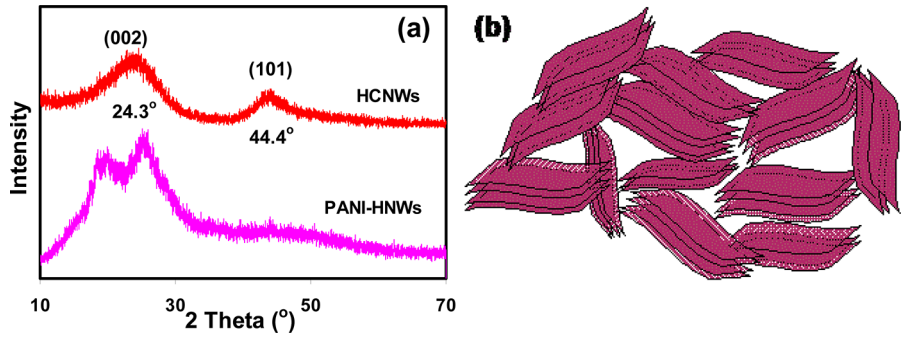

Figure 2. (a) XRD patterns of the PANI-HNWs and HCNWs. (b) Schematic structure of the HCNWs.

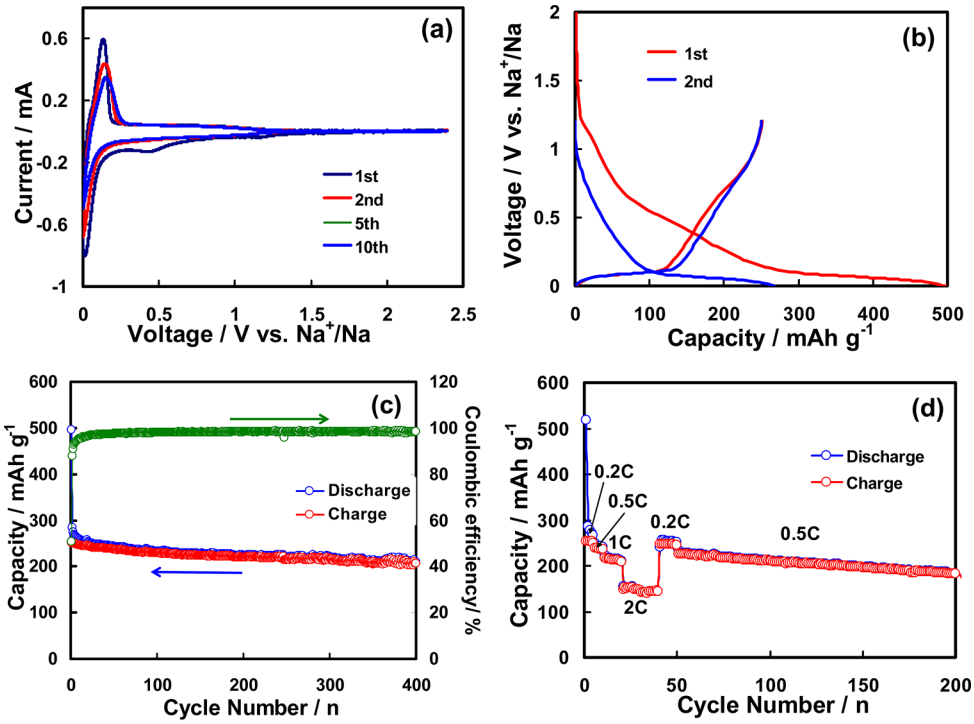

Figure 3. Electrochemical characterization and battery performance of the HCNWs as anode material for Na-ion batteries. (a) CV curves of the HCNW electrode between 0 and 2.5 V at a potential sweep rate of 0.1 mV s^{-1}. (b) First two charge−discharge profiles of the HCNW electrode between 0 and 1.2 V at a current density of 50 mA g^{-1} (0.2 C). (c) Cycle performance of the HCNW electrode at a current density of 50 mA g^{-1} (0.2 C). (d) Discharge capacity of the HCNW electrode as a function of charge−discharge cycles at different charge−discharge current densities of 50 (0.2 C), 125 (0.5 C), 250 (1 C), and 500 (2 C) mAh g^{-1}, respectively.

HCNW electrode cycled in Na-ion electrolyte. During the reduction process, two small irreversible peaks occurred at 1.13 and 0.42 V versus Na^+/Na, which by analogy can be related to the SEI formation, and the two irreversible peaks at different potentials may be attributed to the decomposition of the electrolyte on different active surfaces of the HCNWs. While the Na-ion insertion−extraction behavior in this hard carbon is distinctly different from its Li counterpart (Figure S1, SI), a pair of sharp redox peaks at a lower potential region (0−0.2 V) can be clearly observed, which resemble Li-ion insertion into/extraction out of the graphite structure.[32,33] Additionally, a pair of small and broad redox peaks can be detected in a wide potential range of 0.2−1.0 V. Compared with the lithiation process in hard carbon and graphite, we can infer that the Na-ion insertion−extraction process in the HCNWs takes place in two stages. The reaction occurring at higher potential (0.2−1 V) range is attributed to the charge transfer on the surface of small graphitic clusters, while the reaction occurring at the narrow low potential range (0−0.2 V) is ascribed to Na-ion insertion−extraction in the interlayer of the graphitic microcrystallites.[30] The redox current peaks tend to decrease gradually from the second to fifth cycles (Figure 3a). In the subsequent cycles, the CV curves almost overlap, suggesting that the capacity decay mainly occurs in the first several cycles, and subsequently the electrode shows good Na ion insertion−extraction stability.

The discharge−charge profiles of the HCNWs electrode were measured in the potential range of 0−1.2 V (vs Na^+/Na) at a constant current rate of 50 mA g^{-1} (corresponding to a 0.2 C rate) shown in Figure 3b. The electrode exhibited an initial discharge capacity of 497 mAh g^{-1} and only recovered a charge capacity of 251 mAh g^{-1}, showing a 50.5% initial Coulombic efficiency. The large irreversible capacity loss at the potential range of 1.5−0.4 V (vs Na^+/Na) likely originated from the decomposition of electrolyte partly on the surface of active sites and partly on the carbon surface to form SEI film as discussed

dx.doi.org/10.1021/nl3016957 | Nano Lett. 2012, 12, 3783−3787

above. Based on lessons from Li-ion batteries, the irreversible loss could be reduced in the future by reducing the surface area or the number of surface active sites[32,34] or using additives in the electrolytes.[35,36] The discharge/charge curves can be divided into two distinct stages, which correlate well with the CV curves. The first stage between 1.2 and 0.2 V is characterized by a monotonous slope and a plateau below 0.2 V. It has been shown that the Na-ion insertion into the microvoids formed by the disorderedly assembled graphite microcrystallites takes place at almost 0 V (vs Na^+/Na).[16,18] Thus, this plateau can be attributed to the Na-ion insertion−extraction in the interlayer of the graphite microcrystallites similar to that of Li ions with graphite.[32,33] In comparison, the discharge−charge profiles of the HCNWs in Li-ion electrolyte only display a monotonous slope (Figure S2, SI), in accord with Li insertion−extraction behavior on most of the hard carbons.[30,37]

Figure 3c shows the cyclability of the HCNW electrode at a constant current density of 50 mA g^{-1} (0.2 C rate). The electrode retains a reversible capacity of 206.3 mAh g^{-1} after 400 cycles, corresponding to a capacity retention ratio of 82.2%. The capacity decay mainly happens in the initial 10 cycles, which possibly results from the volume "adjustment" during the Na ion insertion−extraction in the carbon structure. Still, the electrode shows good cycling performance, most likely due to the unique hollow structure which provides a buffering zone for effective release of mechanical stress caused by Na ion insertion−extraction. However, as mentioned above, the electrode shows a very low initial Coulombic efficiency largely due to the high surface area (34.1 m^2 g^{-1}) of the as-prepared HCNWs. This drawback can be lifted by material modification such as surface coating, electrolyte optimization, and the use of highly effective SEI film-forming additives.[38] Nevertheless, after the initial cycle, the Coulombic efficiency of the electrode reached 94% at the fourth cycle and was maintained thereafter at above 98% beyond 10 cycles.

Figure 3d displays the rate performance of the HCNW electrode. This electrode delivered an initial reversible capacities of 252, 238, 216, and 149 mAh g^{-1} at the current rates of 50 (0.2 C), 125 (0.5 C), 250 (1 C), and 500 (2 C) mA g^{-1}, respectively. This result demonstrates that the HCNW electrode exhibits a high rate capability and structural stability even at very high Na-ion insertion−extraction velocities (2 C).

To elucidate the Na ion insertion−extraction mechanism in the HCNW electrode, theoretical simulations on the energy cost for Na-ion insertion into carbon as a function of carbon interlayer distance were carried out. Li-ion insertion simulation was also performed for comparison. The calculation is based on the balance of attractive van der Waals interactions between carbon layers and repulsive interactions between Na or Li ions and carbon. The equilibrium interplanar distance for NaC_6 is about 0.45 nm (Figure 4), while that for LiC_6 is 0.37 nm, in good agreement with the previous experimental observations.[39] It is not surprising that the interplanar distance for NaC_6 is much larger than that of LiC_6 because of the larger size of the Na ion. The calculations of energy cost for Na or Li ion insertion into carbon show that the energy cost curve for Na ion is much steeper than that for the Li ion (Figure 4). For graphite with an interlayer spacing of 0.335 nm, the energy cost for Li-ion insertion is 0.03 eV, while for Na-ion insertion it is 0.12 eV. As the energy of thermal fluctuations at room temperature is 0.0257 eV, thus, Li ions can easily intercalate into graphite layers. Since 0.12 eV is a significant energy barrier

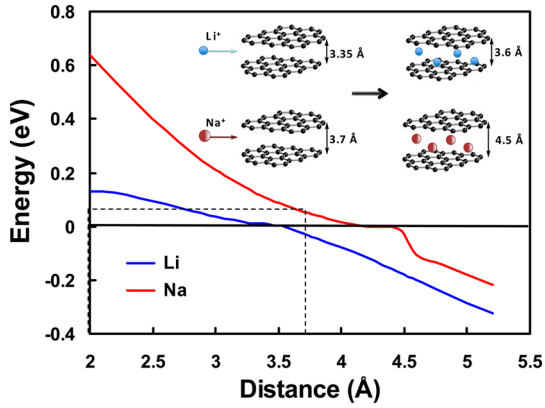

Figure 4. Theoretical energy cost for Na (red curve) and Li (blue curve) ions insertion into carbon as a function of carbon interlayer distance. The inset illustrates the mechanism of Na and Li ions insertion into carbon.

to overcome, Na ions are incapable to intercalate into the graphite layers. However, when the layer spacings increase to 0.37 nm, the energy barrier for Na ion insertion drops markedly to 0.053 eV. This energy barrier is low enough to conquer. The simulation analysis indicates while Na ions cannot intercalate into graphite with an interlayer spacing less than 0.335 nm, they can easily insert into the as-prepared HCNWs with an interlayer spacing of 0.37 nm, consistent with the electrochemical observation. As only a capacity of 10 mAh g^{-1} was obtained from the graphite electrode (see Figure S3, SI), a capacity of 150 mAh g^{-1} was obtained from the HCNW electrode under 0.2 V vs Na^+/Na absolutely deriving from the Na-ion insertion−extraction reaction (Figure 3b). From these experimental and simulation results, it could be speculated that carbon materials with an ordered layer structure and an interplanar distance of a little above 0.37 nm could act a Na-ion insertion anode similar to that of Li-ion with graphite (LiC_6).

In summary, novel HCNWs were synthesized via a two-step method. First, a hollow polyaniline nanowire precursor was obtained by a self-assembly process, and then the precursor was carbonized at high temperature to obtain the target product. When used as anode materials in Na-ion batteries, the HCNW electrode can deliver an initial reversible capacity of 251 mAh g^{-1} and retain 206.3 mAh g^{-1} after 400 cycles at a 0.2 C rate. Even at a high current rate of 2 C, the electrode still can release a reversible capacity of 149 mAh g^{-1}, demonstrating a high rate capability and cyclability. Moreover, the electrochemical characterizations show that Na ions experience two types of insertion−extraction mechanisms: the reaction at a higher voltage range of 0.2−1.0 V is characterized by a charge transfer mechanism on the surface of the small graphitic clusters, while that at a lower voltage range of 0.0−0.2 V is related to Na ion insertion−extraction in the graphitic interlayers. The theoretical simulations show that Na ions can easily insert into layered carbon materials with a layer spacing of 0.37 nm, confirming electrochemical observations.

The development of Na-ion batteries is still in early stages. Although we showed that the nanostructure is helpful for Na-ion insertion, the detailed reaction mechanisms need more careful study, in particular on the nanostructured hard carbon which has more complex structures and reactive sites than graphite. Electrolytes also play an important role in the properties observed, but the effects of composition and additives need to be systematically evaluated and optimized.

dx.doi.org/10.1021/nl3016957 | *Nano Lett.* 2012, 12, 3783−3787

Furthermore, the full cell structure of Na ion batteries may be similar or different from Li ion batteries, depending on the electrodes and electrolytes used. We are currently conducting full cell studies with different designs using the hard carbon nanowires as the anode and hope to report our progress in the future.

■ ASSOCIATED CONTENT

Supporting Information

Experimental details, material characterizations, cyclic voltammograms and charge−discharge voltage profiles of HCNWs electrode in lithium ion electrolyte, charge−discharge profiles of the graphite electrode. This material is available free of charge via the Internet at http://pubs.acs.org.

■ AUTHOR INFORMATION

Corresponding Author

*E-mail: Jun.Liu@pnnl.gov. Phone: +1 5093754443 (J.L.). E-mail: ylcao@whu.edu.cn. Phone: +86 27-68754526 (Y.C.).

Notes

The authors declare no competing financial interest.

■ ACKNOWLEDGMENTS

We thank the support from the U.S. Department of Energy (DOE), Office of Electricity Delivery & Energy Reliability for this research. The theoretical modeling is supported by Basic Energy Sciences, Division of Materials Sciences and Engineering under Award KC020105-FWP12152. Pacific Northwest National Laboratory is a multiprogram national laboratory operated for DOE by Battelle under Contract DE-AC05-76RL01830.

■ REFERENCES

(1) Tarascon, J. M.; Armand, M. *Nature* **2001**, *414*, 359.
(2) Goodenough, J. B.; Kim, Y. *Chem. Mater.* **2010**, *22*, 587.
(3) Tarascon, J.-M. *Nat. Chem.* **2010**, *2*, 510.
(4) Ellis, B. L.; Makahnouk, W. R. M.; Makimura, Y.; Toghill, K.; Nazar, L. F. *Nat. Mater.* **2007**, *6*, 749.
(5) Sauvage, F.; Laffont, L.; Tarascon, J. M.; Baudrin, E. *Inorg. Chem.* **2007**, *46*, 3289.
(6) Doeff, M. M.; Peng, M. Y.; Ma, Y. P.; Dejonghe, L. C. *J. Electrochem. Soc.* **1994**, *141*, L145.
(7) Kim, D.; Kang, S. H.; Slater, M.; Rood, S.; Vaughey, J. T.; Karan, N.; Balasubramanian, M.; Johnson, C. S. *Adv. Energy Mater.* **2011**, *1*, 333.
(8) Cao, Y.; Xiao, L.; Wang, W.; Choi, D.; Nie, Z.; Yu, J.; Saraf, L. V.; Yang, Z.; Liu, J. *Adv. Mater.* **2011**, *23*, 3155.
(9) Barker, J.; Saidi, M. Y.; Swoyer, J. L. *Electrochem. Solid State Lett.* **2003**, *6*, A1.
(10) Caballero, A.; Hernan, L.; Morales, J.; Sanchez, L.; Pena, J. S.; Aranda, M. A. G. *J. Mater. Chem.* **2002**, *12*, 1142.
(11) Wessells, C. D.; Peddada, S. V.; Huggins, R. A.; Cui, Y. *Nano Lett.* **2011**, *11*, 5421.
(12) Wessells, C. D.; McDowell, M. T.; Peddada, S. V.; Pasta, M.; Huggins, R. A.; Cui, Y. *ACS Nano* **2012**, *6*, 1688.
(13) Tepavcevic, S.; Xiong, H.; Stamenkovic, V. R.; Zuo, X.; Balasubramanian, M.; Prakapenka, V. B.; Johnson, C. S.; Rajh, T. *ACS Nano* **2012**, *6*, 530.
(14) Yabuuchi, N.; Kajiyama, M.; Iwatate, J.; Nishikawa, H.; Hitomi, S.; Okuyama, R.; Usui, R.; Yamada, Y.; Komaba, S. *Nat. Mater.* **2012**, DOI: 10.1038/nmat3309.
(15) Qian, J.; Zhou, M.; Cao, Y.; Ai, X.; Yang, H. *Adv. Energy Mater.* **2012**, *2*, 410.
(16) Stevens, D. A.; Dahn, J. R. *J. Electrochem. Soc.* **2000**, *147*, 1271.
(17) Alcantara, R.; Jimenez-Mateos, J. M.; Lavela, P.; Tirado, J. L. *Electrochem. Commun.* **2001**, *3*, 639.
(18) Alcantara, R.; Lavela, P.; Ortiz, G. F.; Tirado, J. L. *Electrochem. Solid State Lett.* **2005**, *8*, A222.
(19) Komaba, S.; Ishikawa, T.; Murata, W.; Yabuuchi, N.; Ozeki, T. *15th International Meeting on Lithium Batteries*, Montreal, Canada, June 27−July 3, 2010; Abstr. No. 793.
(20) Alcantara, R.; Madrigal, F. J. F.; Lavela, P.; Tirado, J. L.; Mateos, J. M. J.; de Salazar, C. G.; Stoyanova, R.; Zhecheva, E. *Carbon* **2000**, *38*, 1031.
(21) Komaba, S.; Murata, W.; Ishikawa, T.; Yabuuchi, N.; Ozeki, T.; Nakayama, T.; Ogata, A.; Gotoh, K.; Fujiwara, K. *Adv. Funct. Mater.* **2011**, *21*, 3859.
(22) Mai, L. Q.; Dong, Y. J.; Xu, L.; Han, C. H. *Nano Lett.* **2010**, *10*, 4273.
(23) Cui, L. F.; Ruffo, R.; Chan, C. K.; Peng, H. L.; Cui, Y. *Nano Lett.* **2009**, *9*, 491.
(24) Cui, L. F.; Yang, Y.; Hsu, C. M.; Cui, Y. *Nano Lett.* **2009**, *9*, 3370.
(25) Park, M. H.; Kim, M. G.; Joo, J.; Kim, K.; Kim, J.; Ahn, S.; Cui, Y.; Cho, J. *Nano Lett.* **2009**, *9*, 3844.
(26) Xiao, L.; Cao, Y.; Xiao, J.; Schwenzer, B.; Engelhard, M. H.; Saraf, L. V.; Nie, Z.; Exarhos, G. J.; Liu, J. *Adv. Mater.* **2012**, *24*, 1176.
(27) Zhang, L. J.; Long, Y. Z.; Chen, Z. J.; Wan, M. X. *Adv. Funct. Mater.* **2004**, *14*, 693.
(28) Guo, X. A.; Fei, G. T.; Su, H.; Zhang, L. D. *J. Phys. Chem. C* **2011**, *115*, 1608.
(29) Zhao, G. Y.; Li, H. L. *Microporous Mesoporous Mater.* **2008**, *110*, 590.
(30) Mochida, I.; Ku, C. H.; Korai, Y. *Carbon* **2001**, *39*, 399.
(31) Ma, Z. F.; Yuan, X. Z.; Li, D.; Liao, X. Z.; Hu, H. P.; Ma, J. Q.; Wang, J. F. *Electrochem. Commun.* **2002**, *4*, 188.
(32) Cao, Y. L.; Xiao, L. F.; Ai, X. P.; Yang, H. X. *Electrochem. Solid State Lett.* **2003**, *6*, A30.
(33) Wang, L. S.; Huang, Y. D.; Jia, D. Z. *Electrochim. Acta* **2006**, *51*, 4950.
(34) Spahr, M. E.; Buqa, H.; Würsig, A.; Goers, D.; Hardwick, L.; Novák, P.; Krumeich, F.; Dentzer, J.; Vix-Guterl, C. *J. Power Sources* **2006**, *153*, 300.
(35) Jeong, S.-K.; Inaba, M.; Mogi, R.; Iriyama, Y.; Abe, T.; Ogumi, Z. *Langmuir* **2001**, *17*, 8281.
(36) Hu, Y.; Kong, W.; Li, H.; Huang, X.; Chen, L. *Electrochem. Commun.* **2004**, *6*, 126.
(37) Gotoh, K.; Maeda, M.; Nagai, A.; Goto, A.; Tansho, M.; Hashi, K.; Shimizu, T.; Ishida, H. *J. Power Sources* **2006**, *162*, 1322.
(38) Zhang, S. S. *J. Power Sources* **2006**, *162*, 1379.
(39) Billaud, D.; Henry, F. X.; Willmann, P. *Mater. Res. Bull.* **1993**, *28*, 477.